Mechanisms of Brine-Side Mass Transfer in a Horizontal Reverse Osmosis Tubular Membrane

The desalination performance of a tubular reverse osmosis membrane was studied under well-defined hydrodynamic conditions. Experimental measurements were made of local mass transfer rates in a 2.31-cm I.D. × 81-cm long horizontal cellulose acetate membrane at 16 locations along the tube length for both laminar and turbulent flows. The membrane's intrinsic permeability to water and NaCl was found to vary significantly along its productive length.

The experiments suggest that the dominant transport mechanisms in laminar flow are forced convection in the upstream region and combined free and forced convection in the downstream region, beyond a distance of approximately 16 tube diameters, for all feed concentrations studied. The Deissler analogy applies well to the turbulent region for $Re \geqq 10^4$; however, it increasingly overpredicts performance as Re is decreased below 10^4.

The experimental results of other workers are interpreted successfully in terms of the mechanisms deduced in the present work.

LEWIS J. DERZANSKY

Clarkson College of Technology
Potsdam, New York 13676

and

WILLIAM N. GILL

Faculty of Engineering and Applied Sciences
State University of New York at Buffalo
Buffalo, New York 14214

SCOPE

Reverse osmosis (also known as hyperfiltration)—which may be classified as a pressure-activated, membrane-moderated, isothermal operation—is a relative newcomer to the chemical engineer's stock of methods for liquid-phase separations. Although it was developed initially for water desalination, reverse osmosis also has found important applications in the food processing, pharmaceutical, paper and pulp, and waste treatment industries. The monographs of Merten (1966), Sourirajan (1970), Kesting (1971), and Lacey and Loeb (1972) contain much information pertaining to the chemistry, engineering, economics and practical aspects of reverse osmosis.

A major obstacle, which may severely limit the performance of reverse osmosis systems, is the phenomenon of concentration polarization. This is the term given to the buildup of a solute layer, adjacent to the membrane surface, which is more concentrated than the feed solution. Concentration polarization is an inherent consequence of the membrane's affinity for transmitting water in preference to solute and is a general phenomenon which occurs, to some extent, in all separation processes. Concentration polarization has several deleterious effects on reverse osmosis: it increases the osmotic pressure at the membrane/brine interface and thereby decreases the effective driving force for water flow through the membrane; it increases the driving force for the transmembrane solute flux and, hence, it increases the salinity of the product water; it can lead to membrane fouling due to precipitation or gelation of sparingly soluble species; and, it may accelerate chemical deterioration of the membrane owing to the higher concentration of aggressive species. Thus, it is necessary to have equations describing the salt buildup in order to make economic appraisals of reverse osmosis. Furthermore, in basic studies, the degree of concentration polarization must be evaluated before the determination of membrane properties can be made.

At steady state, the solute which permeates the membrane is equal to the sum of the bulk flow and diffusive components of the solute flux to the membrane/brine interface. The diffusive component, which is directed from the membrane toward the feed side, is equal to the mass transfer coefficient times the difference between the wall and bulk concentration. Thus, the extent of concentration polarization will depend on the prevailing hydrodynamics and geometry of the system as these factors influence the mass transfer coefficient and increasing the mass transfer coefficient reduces the polarization.

The problem of concentration polarization recently has been reviewed by Gill et al. (1971). With few exceptions (for example, Ramanadhan and Gill, 1969), the existing theories neglect the effects of buoyancy induced convection even though Srinivasan et al. (1967) have suggested that it was present in the early experiments of Merten et al. (1964). Indeed, Hendricks et al. (1972) present experimental evidence for the existence of buoyancy induced instabilities with resulting lower concentration polarization for laminar flow beneath a horizontal membrane sheet.

No data have been reported for horizontal tubular configurations with the carefully controlled hydrodynamics and flow geometry that exist in the present study. Furthermore, by measuring product fluxes at 16 locations along the membrane, one can infer the transport mechanisms which are important and thereby contribute to the development of rational design procedures for reverse osmosis systems, particularly for the horizontal tubular configuration.

CONCLUSIONS AND SIGNIFICANCE

The local behavior of the Sherwood number, as determined from measurements of local product rates and compositions, suggests the following conclusions for fully developed laminar flow:

1. The major transport mechanism in the upstream region of the horizontal reverse osmosis tube is forced convective diffusion which may be described by a uniform wall flux (UWF) Leveque-type model, for which the uncorrected Sherwood number is given by

$$Sh = 1.301 \left[\frac{x}{d_H \cdot Pe} \right]^{-1/3}$$

where x is axial distance, d_H is the tube diameter, and Pe is the Peclet number.

2. After a distance of about 16 diameters, performance was significantly superior to predictions based on the Leveque model and it appears that system behavior is controlled by a combined free and forced convection process which is rather insensitive to Reynolds number and axial distance. Following the analysis of Siegwarth et al. (1969), it was possible to correlate the results in terms of the Rayleigh number Ra by

$$Sh = 0.434\, Ra^{1/4}, \quad Re \simeq 540$$

$$Sh = 0.485\, Ra^{1/4}, \quad Re > 980$$

Correlations of this type, rather than forced convection results, agreed better with the data of Richardson et al. (1969) (desalination of brine) and Monge et al. (1973) and Kennedy et al. (1973) (concentration of sucrose). This is significant because it suggests that previous design methods, which neglect mass transfer enhancement due to ubiquitous buoyancy effects, may give conservative predictions of performance.

For Reynolds number, Re, above about 10^4, the Deissler analogy agreed well with the data:

$$Sh = 0.023\, Re^{0.875}\, Sc^{0.25}$$

where Sc is the Schmidt number. For the transition Re region ($2.3 \times 10^3 < Re < 10^4$), it appears that further studies are required to assess the influence of transverse velocity on the turbulent eddy diffusivity.

In heat transfer to water flowing laminarly in a horizontal tube, several workers (for example, Mikesell 1963; Bergles and Simonds, 1971; Shannon and Depew, 1968) have observed that buoyancy induced secondary flows can enhance the overall heat transfer process markedly when the Grashof number is approximately 10^5. Similarly, in reverse osmosis which is characterized by $Gr_D > 10^5$, solute laden boundary layers, being more dense than the core fluid, may induce angular velocity components which contribute to the transverse mixing of solute. The exact analysis of reverse osmosis systems neglecting buoyancy effects requires the solution of nonlinear coupled partial differential equations since the permeation rate is proportional to the local osmotic pressure which is a function of C_w. The situation becomes more complex when buoyancy effects are included because the secondary velocity components are driven by density differences between the wall and core regions of the flow.

EXPERIMENTAL APPARATUS AND PROCEDURES

The experimental program consisted of 10 series of tests, each corresponding to a different combination of operating pressure and feed concentration. All testing was conducted on the same cellulose acetate membrane (90°C annealing temperature). Feed solutions were made from reagent grade NaCl and distilled water; concentrations included both brackish and sea water salt levels. The operating pressure ranged from less than 4.1 MN/m² (600 lb./sq. in. gauge) to over 5.5 MN/m² (800 lb./sq. in. gauge). For each test series, one high Reynolds number (usually about Re $\simeq$90,000) and several laminar and/or turbulent transition Reynolds number flow runs were conducted. Feed rates were measured with calibrated turbinemeters.

Testing was performed in the high-pressure recirculating reverse osmosis facility schematically shown in Figure 1. Constructed primarily of Type 316 stainless steel wetted parts, the facility can operate at 10.3 MN/m² at room temperature. The heart of the loop is the magnetically-driven Seal/Less centrifugal pump capable of delivering 1.6 liter/s (25 gal./min.) of water at a developed head of 40 m (130 ft.) and with zero leakage. An adjustable stroke diaphragm-type positive displacement pump is used to establish system pressure and, simultaneously, provide make-up to replace the product water forced through the membrane. Pressure pulsations are dampened effectively by a 9.5-liter (2.5 gal.) bladder-type accumulator. Owing to the low efficiency of the magnetic drive, a significant amount of energy is transferred to the loop contents and this heat must be removed. Loop temperature can be controlled to within 0.5°C with a counter-flow double pipe heat exchanger.

The tubular test assembly consists of two stainless steel subsections—the calming section and the reverse osmosis test section—which are lined by a continuous membrane tube. The test section is comprised of an 81 cm. (32 in.) long productive section (that is, the porous walled membrane support tube) whose ends have been concentrically aligned with and welded to specially fabricated transition tubes, approximately 15 cm long (see Figure 2). The internal taper of the transition tube, about 0.5°, was required because it was extremely difficult to build a membrane support tube having an inside diameter exactly matching that of the calming section (the I.D. of

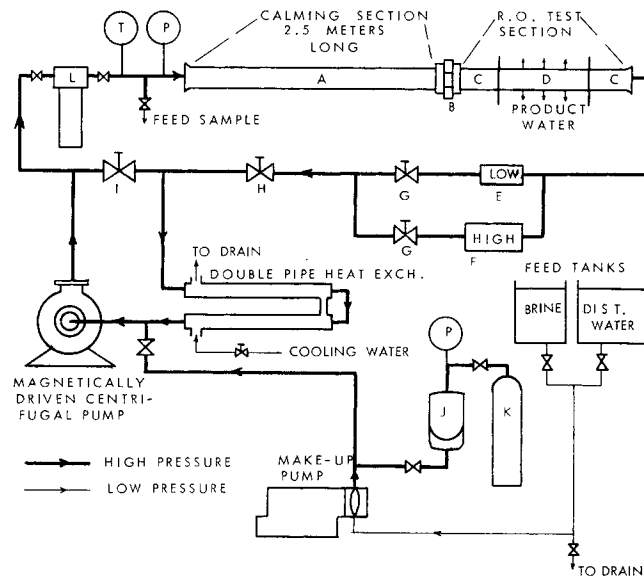

A SEAMLESS 316 SS TUBE 2.54 CM O.D. X 0.124 CM WALL
B PARKER "FERULOK" TUBE CONNECTOR
C TRANSITION TUBE
D POROUS 316 SS MEMBRANE SUPPORT TUBE
E TURBINEMETER, 0.01-0.16 LITER/SEC
F TURBINEMETER, 0.12-1.6 LITER/SEC
G BALL-TYPE ISOLATION VALVE
H GLOBE-TYPE FLOW CONTROL VALVE
I GLOBE-TYPE BYPASS VALVE
J BLADDER-TYPE ACCUMULATOR
K NITROGEN BOTTLE
L 5 MICRON FILTER
P PRESSURE GAGE
T TEMPERATURE GAGE

Fig. 1. Flow diagram of recirculating reverse osmosis facility.

the support tube is approximately 0.38 mm greater than that of the calming section). A Parker Ferulok tube connector, bored out to conform with the inside diameter of the calming section, smoothly joins the upstream end of the reverse osmosis test section (that is, the transition tube) to the calming section. Hence, except for a 37° flare at each end to accommodate the membrane seal, the tubular test assembly is devoid of step changes in inside diameter throughout its 3.66 m length.

The test assembly used in our studies possesses two unique features. First, unlike prior experimenters who have worked with tubes, we have made provision for the establishment of an unobstructed, fully developed velocity profile at the inlet to the reverse osmosis test section by virtue of the more than 100 diameters of calming tube. According to Knudsen and Katz (1958), this length-to-diameter ratio is more than adequate for all Reynolds numbers studied. Second, because the reverse osmosis test section consists of 16 discrete sampling ports (segmented as noted in Figure 2) it is possible to measure axial variations in system performance rather than overall values. Thus, product water, which issues from each collection chamber during a measured time interval, is first weighed (to the nearest 0.1 g.) and then analyzed conductometrically for salt concentration.

The procedures used to install, heat-treat, and seal the ends of the cellulose acetate membrane tube (supplied by Philco-Ford Corporation, Newport Beach, California) were similar to those previously described by Loeb (1966) and Richardson et al. (1969). However, our use of a porous metal support tube, rather than a perforated solid one, eliminated the need for wrapping the membrane in filter paper and/or nylon parchment—a considerable simplification. Further details of the test facility, test section, and assembly techniques may be found in Derzansky (1973).

The membrane was subjected to several hours of high pressure conditioning with distilled water at levels greater than 7.6 MN/m^2 prior to data collection. Consequently, we anticipated, and indeed observed, no evidence of transient behavior due to membrane compaction during the desalination tests. Upon completion of the test program the membrane's thickness was measured along two different sections using a micrometer. That portion of the membrane which lined the calming (nonporous) section of the test assembly had a thickness of approximately 0.22 mm. Within the productive portion of the assembly, the membrane thickness was between 0.13 and 0.15 mm. The as-received (un-annealed) membrane was about 0.24 mm thick. We have estimated that the actual inside diameter d_H of the productive portion of the test section was 2.31 cm.

EXPERIMENTAL RESULTS

Local Membrane Properties

To deduce local brine-side mass transfer characteristics from measurements of product quality and rate, first it is necessary to determine the membrane's water and solute transport properties. Throughout this work, we have used an abridged form of the phenomenological relationships of Sherwood et al. (1967) to describe transmembrane fluxes. Thus, assuming the membrane to be of the solution-diffusion type, that is, no transport through micropores, the following relationships apply (Sherwood et al., 1967):

$$|V_w| = K_1[\Delta P - \Delta\pi] = K_1[\Delta P - K_5(C_w - C_p)] \quad (1)$$

$$n_s = K_3\,\rho(C_w - C_p) \quad (2)$$

The product salt concentration can be expressed in terms of the salt concentration at the brine-membrane interface by first noting that, from a steady state salt balance,

$$C_p = \frac{n_s}{n_s + \rho|V_w|} \quad (3)$$

Simultaneous solution of Equations (1) through (3) gives

$$2C_p = (\gamma\Delta P - C_w + \kappa) + [(\gamma\Delta P - C_w + \kappa)^2 + 4\kappa C_w]^{1/2} \quad (4)$$

where

$$\gamma = \frac{K_1}{(K_1 K_5 - K_3)}$$

$$\kappa = \frac{K_3}{(K_1 K_5 - K_3)}$$

Since the permeability constants, K_1 and K_3, depend on a variety of chemical, manufacturing, annealing, and operating variables (Richardson et al., 1969), it is virtually impossible to obtain accurate values of them prior to actually using the membrane. Hence, they must be determined, in situ, under conditions which are nearly identical to those existing during test runs. Consequently, for each test series, the membrane was calibrated by recirculating a highly turbulent feed solution whose composition, temperature, and pressure were essentially the same as in the low Reynolds number runs. For high Reynolds numbers it is assumed that Brian's (1966) turbulent flow formula is valid:

$$(C_w - C_p) = (C_o - C_p)\exp\left\{\frac{|V_w|\,d_H}{D\,Sh}\right\} \quad (5)$$

where Sh is the Sherwood number for the limiting case of zero transverse velocity and was obtained from the Deissler (1955) analogy,

$$Sh = 0.023\,Sc^{.25}\,Re^{.875} \quad (6)$$

Thus, with V_w, C_o, and C_p determined from experimental measurements and Sh calculated from Equation (6), C_w is calculated from Equation (5). Then, Equations (1) and (2) are used to find K_1 and K_3, respectively, since ΔP is known and K_5 can be obtained from Richardson et al. (1969) or Johnson et al. (1966). Since C_w/C_o was calculated to be always less than about 1.05 for the calibration conditions employed in this study, the dependence of the permeability constants on the accuracy of Equations (5) and (6) should be very small.

Note that these calculations were performed for each of the 16 sampling ports, that is, the K_{1i} and K_{3i}, i = 1 to 16, were evaluated for each test series. A typical set of membrane properties is shown in Table 1 where it is seen that port to port variations do, indeed, exist. The reason for this may be due, partially, to differences in the degree of membrane stress as the membrane conforms to the larger diameter of the porous support tube which, owing to the manufacturing method, undulates very slightly along its length. Another possible contributing factor may be related to the nonuniform permeability of the porous stainless steel support tube. For instance, preliminary tests (performed prior to insertion of the membrane) revealed that the local permeability of the porous support tube differed by several hundred percent between certain ports. Consequently, the transpiration velocities during the low pressure heat-treatment process can vary significantly along the membrane. This may lead to differing degrees of polymer crystallinity in the membrane's active layer. Recently, Grethlein (1973) has shown that even under carefully controlled conditions, variations within a given membrane still exist.

Effect of Reynolds Number on Performance

As the feed Reynolds number is changed from a turbulent to a laminar value we would expect the system's performance initially to be primarily controlled by the membrane's resistance and then by a combination of brine-side boundary layer and membrane resistances. That is, the lower the Reynolds number, the poorer the overall rate and quality of the product water. Table 2 shows how the local product mass and composition are affected by feed

Reynolds number when all other operating parameters are kept nearly constant. (Recall, from Figure 2, that ports 1 through 8, 9 through 12, and 13 through 16, have nominal lengths of 2.54, 5.08, and 10.2 cm, respectively.) Note that for the two highest *Re* runs, with the exception of the first two ports, local product rate and quality deteriorate only by roughly 1% and 6%, respectively, as *Re* decreases from 51,300 to 20,530. This relative insensitivity of system performance to *Re*, even though *Re* has decreased by 60%, is due to the small fraction of the overall resistance attributable to the brine-side boundary layer when the feed is in fully-developed turbulent flow. When the Re is decreased to 5,130, the flow is now within the turbulent transition region wherein the intensity of turbulent transfer processes diminishes and is more sensitive to *Re*. Comparing local performance at $Re = 5{,}130$ to that at $Re = 51{,}300$, we note a decrease of approximately 4 to 8% in product rate and 30 to 40% in quality, except again, for ports 1 and 2 which have deteriorated less. A further decrease in feed flow rate to $Re = 2{,}053$, just within the laminar region, results in about an 18% decrease in product rate and more than a 100% increase in product salinity for those ports beyond the first 10 cm as compared to those at $Re = 51{,}300$. This dramatizes the marked decrease in brine-side mass transfer resulting from operating in the laminar regime. The relatively better performance in the upstream ports is due to the larger mass transfer coefficients characteristic of the entry region. Finally, the performance at $Re = 1{,}026$ is important because it reveals the interesting result that from the fifth port onwards the

Table 1. Local Membrane Properties

Calibration run for Test Series III

$Re = 51{,}300$

$C_0 = 0.142$ normal (8,300 ppm NaCl)

$\Delta P = 662$ lb./sq.in. (4.43 MN/m²),

$\pi_0 \simeq 99$ lb./sq.in., $T = 27.0°C$

Port number	Pure water permeability $10^7 \times K_1$, cm/s · lb./sq. in.	Solute permeability $10^5 \times K_3$, cm/s	1-Rejection $(1 - R)$
1	7.34	5.22	0.1106
2	7.19	3.91	0.0871
3	8.85	4.78	0.0867
4	8.73	4.46	0.0825
5	8.92	5.10	0.0913
6	9.07	5.29	0.0928
7	9.68	5.13	0.0853
8	8.15	4.72	0.0922
9	9.06	5.21	0.0917
10	8.79	5.10	0.0924
11	8.92	5.31	0.0946
12	9.15	5.05	0.0884
13	8.57	4.84	0.0902
14	8.46	4.54	0.0862
15	8.85	5.05	0.0912
16	8.18	6.29	0.1184

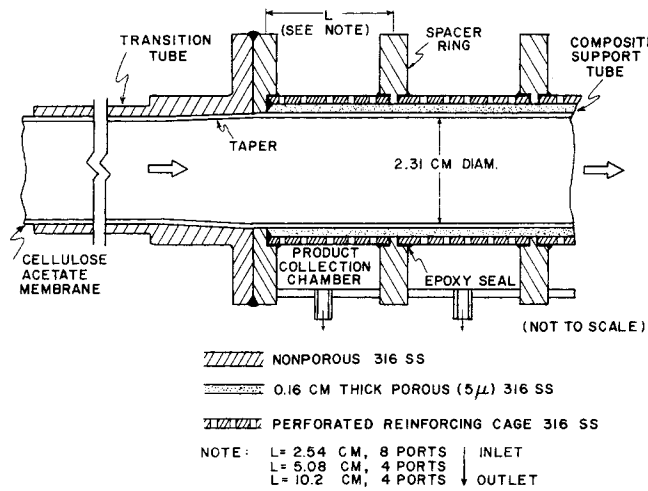

Fig. 2. Reverse osmosis test section details.

Table 2. Desalination Performance: Local Product Mass and Quality
Temperature: 27°C, Collection time: 50 minutes
Test Series III

Pressure, lb./sq.in.gauge (MN/m²)	662 (4.56)		659 (4.54)		661 (4.55)		662 (4.56)		662 (4.56)	
Reynolds number	51,300		20,530		5,130		2,053		1,026	
Port number	Grams	Normality	Grams	Normality	Grams	Normality	Grams	Normality	Grams	Normality
1	22.8	0.0163	22.9	0.0167	22.5	0.0178	21.6	0.0204	21.1	0.0212
2	23.0	0.0128	23.0	0.0130	22.3	0.0151	21.0	0.0197	20.2	0.0211
3	28.4	0.0129	28.2	0.0136	26.8	0.0164	24.4	0.0229	23.7	0.0244
4	28.6	0.0123	28.2	0.0130	27.0	0.0164	24.6	0.0239	23.5	0.0247
5	28.9	0.0136	29.2	0.0140	27.6	0.0182	24.4	0.0269	23.9	0.0273
6	29.2	0.0138	28.8	0.0145	27.3	0.0189	24.1	0.0289	24.0	0.0284
7[a]	30.7	0.0127	29.7	0.0134	27.6	0.0177	24.5	0.0265	24.2	0.0263
8[a]	26.0	0.0137	26.2	0.0143	25.1	0.0190	22.0	0.0290	21.9	0.0287
9	56.6	0.0136	56.1[b]	0.0143	52.1	0.0192	45.9	0.0290	45.4	0.0287
10	55.5	0.0137	55.0	0.0144	52.0	0.0193	45.8	0.0291	45.2	0.0288
11	56.3	0.0141	55.4	0.0149	52.2	0.0202	45.9	0.0306	45.0	0.0302
12	57.7	0.0132	57.1	0.0138	53.4	0.0186	47.0	0.0283	46.3	0.0281
13	108.4	0.0134	107.3	0.0141	100.1	0.0189	88.5	0.0286	86.7	0.0287
14	107.0	0.0128	106.1	0.0135	99.4	0.0183	87.6	0.0281	85.4	0.0283
15	111.9	0.0135	110.4	0.0142	103.7	0.0193	90.9	0.0300	89.4	0.0302
16	102.5	0.0175	101.5	0.0184	95.7	0.0237	84.1	0.0360	82.9	0.0362
Feed	—	0.142	—	0.140	—	0.138	—	0.136	—	0.133

[a] Suspected interport leakage.
[b] Estimated.

local product behavior is essentially the same as the run at $Re = 2{,}053$, even though the feed flow rate differs by a factor of two. This is unexpected if one anticipates that brine-side mass transfer is of the forced-convection (Leveque) type. Other test runs (Derzansky, 1973) reveal the same insensitivity of laminar performance to Reynolds number, even for $Re \simeq 500$. In order to obtain a sharper indication of the local transport phenomena, it is necessary to extract from the data information which reflects the brine side mass transfer characteristics and is less obscured by the axial variations of K_1 and K_3. For this purpose we have computed local Sherwood numbers $Sh^\bullet$ given by

$$Sh^\bullet \equiv \frac{k^\bullet d_H}{D} \tag{7}$$

where the mass transfer coefficient $k^\bullet$ is defined as

$$k^\bullet \equiv \frac{\vec{j}_s}{\rho(C_w - C_o)} = \frac{-D\dfrac{\partial C}{\partial y}(x, 0)}{(C_w - C_o)} \tag{8}$$

We now apply Fick's first law of diffusion (Bird et al., 1960) at the membrane/solution interface,

$$n_s = -\rho D \frac{\partial C}{\partial y}(x, 0) + \rho V_w C(x, 0). \tag{9}$$

The left-hand side of Equation (9) represents the mass flux of salt with respect to the stationary membrane surface. Since no separation occurs on the product side of the membrane, no transverse concentration gradients exist there so that $n_s = \rho V_w C_p$ and Equation (9) can be rewritten as

$$|V_w|(C_w - C_p) = -D\frac{\partial C}{\partial y}(x, 0) \tag{10}$$

since V_w is in the negative y-direction (see Figure 3). Substituting Equation (10) into Equation (8) gives the working expression for $k^\bullet$,

$$k^\bullet = \frac{|V_w|(C_w - C_p)}{(C_w - C_o)} \tag{11}$$

$Sh^\bullet$ is evaluated from known values of d_H and D and measured V_w, C_p, and C_o, together with the calculated value of C_w, which is obtained from Equation (2) using the relation $n_s = \rho V_w C_p$ and the local calibrated value of K_3.

It is important to keep in mind the fact that $Sh^\bullet$ is not the same as the conventional Sherwood or Nusselt numbers, Sh and Nu, which apply to systems for which the transverse velocity is negligible at the wall. The superscript dot signifies that these quantities take into account the effect of V_w on the mass transfer coefficient due to distortion of the velocity and concentration profiles in the vicinity of the membrane's surface (Bird et al., 1960).

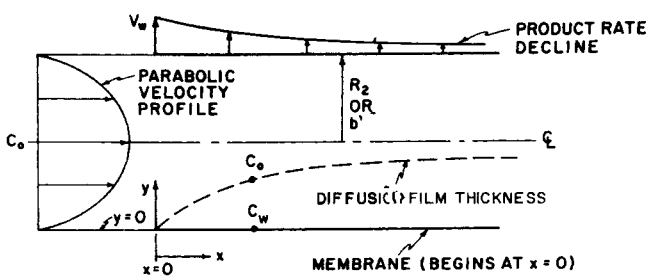

Fig. 3. Coordinate system showing fully developed laminar profile and performance characteristics for a uniform membrane.

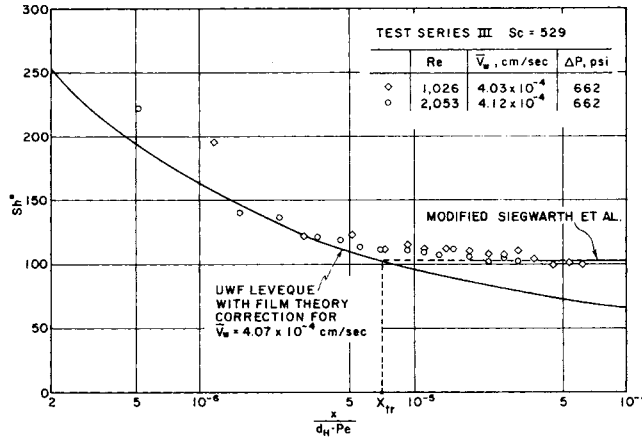

Fig. 4. Experimental Sherwood number vs. dimensionless axial distance for Test Series III. (Laminar flow, $\pi_0 \simeq 92$ lb./sq.in., $C_0 \simeq 0.134$ normal).

Laminar Flow Sherwood Numbers

In Figure 4 the laminar flow data of Table 2 are presented in $Sh^\bullet$ form. The abscissa represents the dimensionless axial coordinate conventionally used for forced convective transport. The solid curve labeled *UWF Leveque With Film Theory Correction* represents an approximate theoretical prediction for $Sh^\bullet$ behavior which is based upon a Leveque-type (that is, $Sh = 1.301\left(\frac{x}{d_H \cdot Pe}\right)^{-1/3}$) transfer mechanism modified for the presence of a uniform transverse velocity by the rate factor-correction factor concept of film theory (Bird et al., 1960). Note that the upstream experimental $Sh^\bullet$'s fall close to the aforementioned predictions with the $Re = 2{,}053$ run agreeing up to the first 20 cm (ports 1 through 8) and the $Re = 1{,}025$ run for the first 10 cm (ports 1 through 4). It should be realized that had the abscissa been simply x/d_H, then the data points would nearly coincide for $x/d_H \gtrsim 8$, indicating that $Sh^\bullet$ is virtually independent of Re in this region. As it is, however, the data of the $Re = 1{,}025$ run are shifted towards the right. Note, too, that the variation in local membrane properties is still evident as reflected by the scatter of the $Sh^\bullet$ values. Had the membrane been uniform throughout the test section, the data points would have scattered less. Nevertheless, it is clear that in the downstream portion of the test section $Sh^\bullet$ values are significantly greater than those predicted using the modified Leveque model for uniform wall flux. Furthermore, it is apparent that the last four data points, corresponding to ports 13 through 16 which comprise half of the test section's length, have nearly identical $Sh^\bullet$ values for both runs. This suggests that an asymptotic region exists beyond a short distance from the inlet in which the mass transfer processes become insensitive to both Re and location within this region.

The other test series which were conducted gave similar laminar behavior when $Re > 980$. However, a number of runs performed at $Re \approx 500$ showed a small decrease in $Sh^\bullet$ for the downstream region, about 5 to 10% smaller than for $Re > 980$. Nevertheless, these experimental downstream $Sh^\bullet$ values were still significantly greater than predicted by forced convection theory. In all laminar runs, the observed local desalination performance was equal to or better than the predictions based on a forced convection transport model. As will be demonstrated, such be-

havior is suggestive of combined free and forced convection transfer mechanisms.

Turbulent Flow Sherwood Numbers

In Figure 5 we have presented Sh^* data of Test Series VI (Derzansky, 1973) for which Reynolds numbers extend from the laminar limit up into the transitional turbulent flow range. Notice that the abscissa represents the number of tube diameters to the mid-point of a sampling port. It is seen clearly that the Reynolds number exerts a strong influence on Sh^* throughout the test section in contradistinction to the behavior depicted in Figure 4 for laminar flow. Also, it is possible to discern an entry length beyond which the turbulent Sh^* assumes a fully developed value. For the single laminar run shown in Figure 5, we again observe that the upstream portion of the test section (say up to $x/d_H = 8$) is consistent with a forced-convection mechanism, but that the remainder exhibits mass transfer performance superior to this mode.

DISCUSSION OF RESULTS

To correlate experimental reverse osmosis data effectively it is important to have available an accurate but manageable theoretical model. Since the membrane exhibited significant axial variation in its pure water and solute permeabilities (see Table 1), use of accurate series solutions such as those developed by Gill et al. (1966a, b) and by Shaw et al. (1972) for laminar flows were ruled out because they assume uniform membrane properties, K_1 and R. Furthermore, they require considerable numerical computation. Therefore, recourse was made to the film theory model (Bird et al., 1960) which has previously been shown to provide a simple yet accurate method for describing concentration polarization in laminar (Kimura and Sourirajan, 1968; Derzansky, 1973) and turbulent (Gill et al., 1971) reverse osmosis systems. Consequently, the hypothetical uncorrected Sherwood number Sh in the limiting case of zero interfacial velocity was back-calculated from Sh^*. Only data obtained from ports 13 through 16 were so treated since they are in the fully developed region for turbulent flows and the asymptotic, Re-insensitive region for laminar flows.

Briefly, the relationship between Sh^* and Sh according to film theory is given by (Bird et al., 1960)

$$Sh^* = \theta_{AB} \cdot Sh \tag{12}$$

where

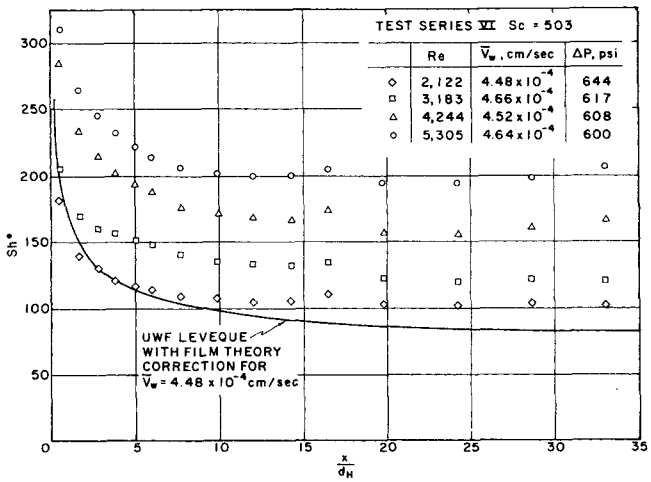

Fig. 5. Experimental Sherwood number vs. dimensionless axial distance for Test Series VI. (Laminar and transition region flow, $\pi_0 \simeq 62$ lb./sq.in., $C_0 \simeq 0.09$ normal).

$$\theta_{AB} = \frac{\phi_{AB}}{e^{\phi_{AB}} - 1} = \frac{Pe_w/Sh}{e^{(Pe_w/Sh)} - 1} \tag{13}$$

and

$$Pe_w = -|V_w|\, d_H/D$$

Substituting Equation (13) into (12) and then rearranging and taking logarithms, we obtain

$$Sh = \frac{Pe_w}{\ln\left(1 + \dfrac{Pe_w}{Sh^*}\right)} \tag{14}$$

Equation (14) was used to convert the local Sh^* results for each test condition into corresponding Sh values, that is, it accounts for the measured local (port-averaged) value of interfacial velocity V_w.

Laminar Results

As indicated earlier, the downstream laminar behavior suggests the presence of an additional transport mechanism, not accounted for in the UWF Leveque-film theory model, which enhances local mass transfer between the membrane surface and the bulk feed stream. This mechanism is free convection. The argument for the existence of significant buoyancy effects in our experiments is supported by the literature dealing with combined free and forced convection laminar flow heat transfer in horizontal tubes. For instance, Shannon and Depew (1968) have observed Nusselt numbers which were up to 150% greater than the Graetz-type predictions for the case of heating water at a Grashof number of 10^5 (our Gr_D is of the order 10^6). Bergles and Simonds (1971) also have found similar effects in their experiments with water. Dye tracer experiments conducted by Mikesell (1963), Bergles and Simonds (1971), and others have shown conclusively that density variations, between the wall region fluid and the bulk, give rise to secondary spiral-like flows which are symmetric with respect to a vertical plane through the tube axis. In reverse osmosis, owing to the difference in salt concentration between wall and bulk regions, analogous density variations exist.

To date, no theoretical analysis of reverse osmosis in horizontal tubes with laminar combined free and forced convection has appeared in the literature. However, several analyses of a similar heat transfer problem do exist. Of special interest here is the boundary layer analysis of Siegwarth et al. (1969) since it is applicable to fluids of large Prandtl number and constant viscosity. Siegwarth et al. have considered the special case where simultaneously the wall heat flux is axially uniform and no circumferential temperature gradients exist in the wall. Under these conditions it is found that the perimeter-averaged Nusselt number takes on an asymptotic value given by

$$Nu = 0.561\, Ra^{1/4} = 0.561\left[\frac{g\beta d_H^3 (T_w - T_b)}{\nu^2} \cdot \frac{\nu}{\alpha}\right]^{1/4} \tag{15}$$

Importantly, Nu is predicted to be independent of Reynolds number when Re is sufficiently large for the assumptions in the analysis to hold.

Newell and Bergles (1970) have demonstrated, by finite-difference calculations, that the boundary conditions used by Siegwarth et al. (1969) give larger Nu values than the case where there is uniform wall heat flux but in which circumferential temperature gradients do exist in the wall. Although the computations of Newell and Bergles were performed specifically for water which has a Prandtl number around 10, their findings are probably qualitatively valid for higher Prandtl numbers too. This suggests that the coefficient in Equation (15) should

be smaller in the case of reverse osmosis where it is not possible to impose circumferentially uniform wall concentrations because a nonuniform angular velocity field exists which is coupled to the wall concentration. This is in contrast to the heat transfer case where one can control the wall temperature by external means.

Guided by Equation (15), the laminar Sh values were correlated in the form

$$Sh = \text{constant} \cdot Ra^{1/4} = C_1 \cdot (Gr_D \cdot Sc)^{1/4} \quad (15a)$$

where, for mass transfer,

$$Gr_D = \frac{g\zeta d_H^3 (C_w - C_o)}{\nu^2}$$

Note that we have used C_o rather than C_b since only a very small fraction of the feed was removed as product in our tests. The value of the volumetric expansion coefficient (due to concentration change) ζ was estimated to be 0.70 from the densities of NaCl solutions given in Hodgman (1962).

As implied earlier, the downstream Sh^*'s for those tests having $Re \simeq 534$ were somewhat lower than the Sh^*'s for $980 \leqq Re \leqq 2{,}166$. Therefore, we determined a least-square value of C_1 separately for the two Re ranges. The final results are

$$Sh = 0.434\, Ra^{1/4}, \; Re \simeq 534 \quad (16)$$

and

$$Sh = 0.485\, Ra^{1/4}, \; 980 \leqq Re \leqq 2{,}166. \quad (17)$$

Equation (16) is based on data from ports 13 through 16 for four runs which had $525 \leqq Re \leqq 541$. The experimental Sh's for these runs had average and maximum deviations from Equation (16) of 4.73% and −16.9%, respectively. Equation (17) was obtained from seventeen laminar runs having $Re \geqq 980$. Corresponding deviations from Equation (17) are 2.56% and −8.71%.

For illustration, we have calculated Sh^* by using Equations (12), (13), and (17) together with the experimental values of Pe_w and Ra for each of the last four ports of the laminar runs of Test Series III (see Table 2). It was found that the predicted Sh^*'s all were within ± 2.4% of their collective mean ($Sh^*_{mean} \simeq 104$) so that we have indicated only Sh^*_{mean} in Figure 4 and labeled it *modified Siegwarth et al.* For practical purposes, we note that all of the data points are adequately bracketed by the UWF Leveque curve in the inlet region and the modified Siegwarth et al. curve for the downstream region. Such behavior is consistent with the notion that the important mechanisms responsible for brine-side laminar mass transfer are associated, in the initial section of the tube, with forced convective diffusion and, further downstream, with combined free and forced convection which is rather insensitive to Reynolds number or distance.

Turbulent Results

Unlike the laminar flow results, the turbulent data indicate that the local product quality always improves as Re increases. Such behavior is expected since it is well known that the eddy-diffusivity and, hence, the mass transfer coefficient, increases with Re.

It is of interest, however, to determine the range of applicability of conventional turbulent Sherwood number correlations, that is, the Deissler analogy and the Chilton-Colburn analogy. Since these analogies relate to the fully developed region, we have considered data from the downstream half of the test section in the following comparison (note the relative constancy of Sh^* for the last four data points of each turbulent run shown in Figure 5). Figure 6 presents the results of nine turbulent runs (calibration runs excluded) in which Sc ranged between 503 and 600 (see Derzansky, 1973 for complete test conditions). Each data point represents the average of four downstream Sh values, obtained through Equation (14), divided by Sc to the one-third power (Chilton-Colburn) or one-fourth power (Deissler). The symbols with and without flags are associated with the Chilton-Colburn and Deissler analogies, respectively. The form of each analogy is indicated on Figure 6. The data points for $Re = 49{,}000$ are not as reliable as the remaining points since in calculating their value it was necessary to take the difference between two numbers of nearly equal magnitude. Thus, we conclude that the Deissler analogy is preferable to the Chilton-Colburn analogy for high Sc systems providing $Re \geqq 9{,}800$.

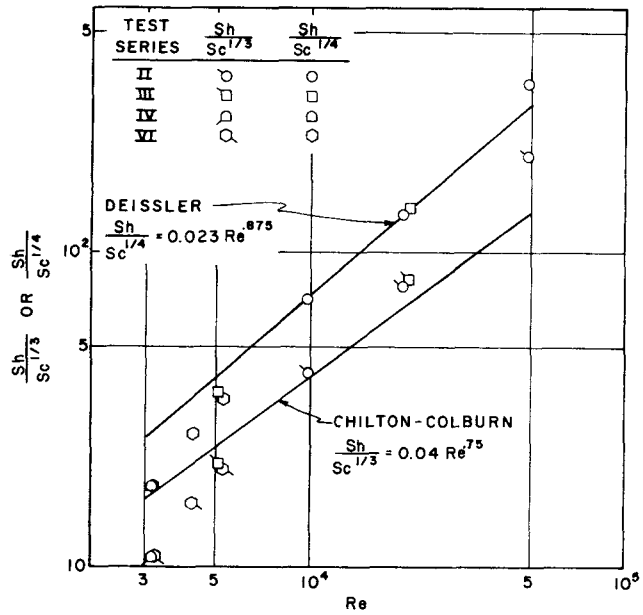

Fig. 6. Comparison of experimental downstream Sherwood numbers, for fully-developed and transitional turbulent flow, with Chilton-Colburn and Deissler analogies. Test Series II, III, IV, and VI correspond to the following Schmidt number—applied pressure drop (lb./sq.in.) pairs, respectively: 600, 835; 529, 660; 516, 818; 503, 608.

In the transition range, $Re < 9{,}800$, both correlations increasingly overpredict the data and neither appears satisfactory. It is interesting to note, however, that the few results which were obtained in the transition region were found to exhibit the same trend as predicted by Derzansky (1968). Derzansky (1968) performed a Graetz-type analysis and employed the eddy-diffusivity function proposed by Gill and Scher (1961). This eddy-diffusivity function adequately accounts for the observed friction factor-Reynolds number behavior in the transitional region of pipe flow.

APPLICATION OF RESULTS

At this point we shall demonstrate how the experimental findings of this study may be used to estimate the tube length beyond which desalination performance is influenced by combined free and forced convection. We note from Figure 4 that by extending the Siegwarth et al. line until it intersects the UWF Leveque curve, we can obtain an effective dimensionless transition length X_{tr}. Actually, there exists a short transition region in which the dominant mass transfer mechanism changes continuously, rather than abruptly, from conventional forced convective diffusion to that of combined free and forced convection. Nevertheless, it is reasonable to expect that for tubes longer than $d_H Pe X_{tr}$ desalination performance will exhibit the bene-

ficial effects of buoyancy induced convection.

X_{tr} is evaluated by equating the two expressions for Sh:

$$1.301(X_{tr})^{-1/3} = C_1\left(\frac{g\zeta d_H^3}{\nu D}\right)^{1/4}(C_w - C_o)^{1/4} \quad (18)$$

(UWF Leveque) (Siegwarth et al.)

Note that the Leveque Sh decreases with axial distance to the 1/3 power and is independent of concentration level whereas the Siegwarth et al. Sh is independent of distance but, since it accounts for buoyancy effects, depends on the concentration level. The value of C_w must be determined for each set of operating conditions (C_o, d_H, ΔP), fluid properties (D, ν, ζ), and membrane characteristics (K_1, K_3). Hence, using Equations (7), (11), and (12), we may obtain

$$\frac{C_w - C_p}{C_o - C_p} = \exp\left\{\frac{|V_w|d_H}{DC_1\left(\frac{g\zeta d_H^3}{\nu D}\right)^{1/4}(C_w - C_o)^{1/4}}\right\} \quad (19)$$

where V_w and C_p satisfy Equations (1) and (4). For specified operating conditions, one guesses a value for C_w and calculates corresponding values of C_p and $|V_w|$ in that order. This set of C_w, C_p, and $|V_w|$ values is substituted into Equation (19) to determine whether both sides are identical. If not, a new guess is made for C_w and the scheme is repeated until an identity results. Due to the complex and coupled nature of Equations (1), (4), and (19), it was necessary to use a systematic forward and backward marching technique in which the step size of C_w decreased by a factor of ten each time the marching direction reversed. Upon convergence to the C_w root of Equation (19), the values of C_w and C_o are substituted into Equation (18) to solve for X_{tr}. Observe that the proportionally constant C_1, of the Siegwarth et al. correlation, also influences the final result.

For illustrative purposes, we have computed X_{tr} for ranges of NaCl feed concentrations C_o, tube diameters d_H, and cellulose acetate membrane properties K_1 and K_3, which correspond to brackish and ocean waters, commercial tube sizes, and "tight" and "open" membranes, respectively. Physical properties of the fluid were assumed to be independent of concentration and were as follows: $D = 1.6 \times 10^{-5}$ cm²/s; $\nu = 0.009$ cm²/s; $\zeta = 0.70$. In order to obtain a somewhat conservative estimate of X_{tr}, we have taken $C_1 = 0.4$.

Figures 7 and 8 show the results of our computations for X_{tr} for "tight" and "open" membranes, respectively. Notice that for a given feed concentration X_{tr} increases very significantly as d_H decreases and as the operating pressure decreases. This occurs because Ra is proportional to d_H^3 so that a 50% reduction in d_H gives a Ra which is one-eighth the original value and, thus, diminishes the importance of combined free and forced convection. Decreasing the operating pressure decreases $|V_w|$ so that C_w is reduced which also reduces Ra. It appears that for the tight membrane at 600 lb./sq. in. gauge a shallow minimum occurs at about 15,000 ppm NaCl. In general, though, X_{tr} is relatively insensitive to C_o for, say, $C_o >$ 10,000 ppm NaCl for the ranges of parameters used here. However, for all cases studied, X_{tr} is predicted to increase rapidly as C_o approaches values typifying dilute brackish waters.

On the basis of Figures 7 and 8, one may speculate that the beneficial effects of buoyancy-induced mass transfer enhancement will occur over larger sections of the tube for high operating pressures and high feed concentrations. These are precisely the operating conditions which apply for seawater desalination. Hence, we should look upon

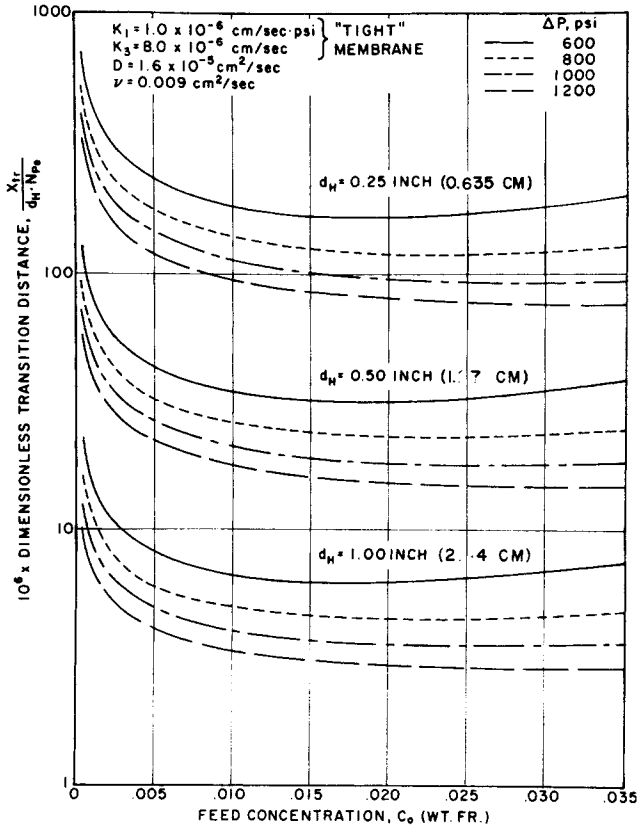

Fig. 7. Estimated dimensionless transition distance for onset of combined free and forced convection vs. feed concentration for NaCl-H_2O desalination using a tight membrane.

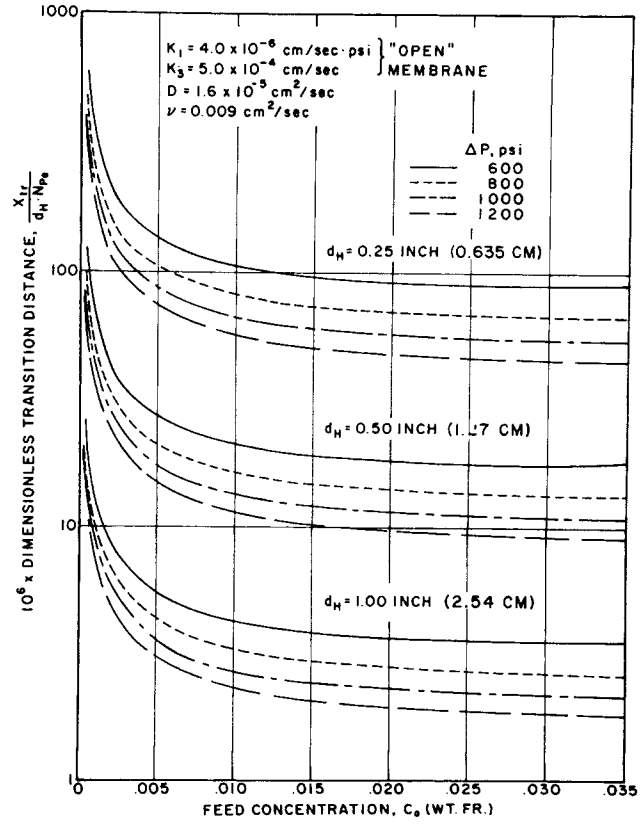

Fig. 8. Estimated dimensionless transition distance for onset of combined free and forced convection vs. feed concentration for NaCl-H_2O desalination using an open membrane.

Table 3. Comparison of Data of Richardson et al. (1969) with Predictions of Forced Convection Models Which Neglect or Include Buoyancy Effects

Membrane specifications: I.D. = 2.26 cm, Length = 61 cm
Calculated constants: $K_1 = 1.72 \times 10^{-6}$ cm/s · lb./sq.in.
$K_3 = 3.94 \times 10^{-5}$ cm/s
Operating pressure (gauge): 800 lb./sq.in.gauge (5.51 MN/m²)
Feed properties: $C_0 = 10{,}150$ ppm NaCl, $\pi_0 = 117$ lb./sq.in. (0.805 MN/m²)
$\rho = 1.0$ g/cm³, $\nu = 0.0089$ cm²/s
$Sc = 585$

Reynolds number, Re	Overall product rate, gal./day/sq.ft. FC followed by CFFC*			Overall salt reduction, (C_0/C_p) FC followed by CFFC*			x_{tr}, cm
	FC† only		Exp't.	FC† only		Exp't.	
19,284	—	—	23.3	—	—	21.7	—
2,143	16.1	16.6	17.1	6.29	6.74	7.1	29.2
1,714	15.6	16.4	16.6	5.86	6.55	6.7	23.4
1,286	15.0	16.2	16.6	5.35	6.37	6.3	17.5
857	14.0	16.0	15.9	4.71	6.19	5.9	11.7
429	12.5	15.8	15.0	3.80	6.01	5.2	5.8

† FC = forced convection, that is, $Sh = 1.301 \left(\frac{d_H}{x} Pe\right)^{1/3}$.

* CFFC = combined free and forced convection, that is, $Sh = 0.42\ Ra^{1/4}$.

this application of reverse osmosis with somewhat more optimism, at least from a mass transfer standpoint.

Interpreting Experiments of Other Investigators on the Basis of Combined Free and Forced Convection

The major finding deduced from the laminar flow experiments described earlier is that, even for moderate tube lengths, buoyancy effects arise which significantly enhance brine-side mass transfer rates. However, this contention is based on a rather limited range of experimental parameters, that is, tube diameter = 2.31 cm and Schmidt numbers between 478 and 600. Consequently, it would be desirable to examine the experimental results of other workers to determine whether or not they, too, suggest the existence of combined free and forced convection.

Although several investigators have reported data for tubular reverse osmosis systems, most of this work considered the turbulent flow regime and/or was performed on ion-exchange type membranes which are notorious for their concentration-dependent solute rejections (Thomas, 1972). Fortunately, Richardson et al. (1969) (at the Philco-Ford Corporation) and a group at the University of California, Davis (Monge et al., 1973; Kennedy et al., 1973) have presented laminar flow data for sodium chloride and sucrose feed solutions, respectively, using cellulose acetate membranes. However, their measurements were of overall product rates and concentrations rather than local values and, also unlike the present study, neither Richardson et al. nor the UC Davis workers made provisions for ensuring an unobstructed, fully-developed inlet velocity profile. Therefore, it is not possible to pinpoint the axial distances at which buoyancy effects occur. Nevertheless, as will be shown, the experimental results of Richardson et al. and the UC Davis group are more consistent with a model allowing for both forced convection ($X < X_{tr}$) and combined free and forced convection ($X > X_{tr}$) than they are with a model which excludes the latter.

The Philco-Ford experiments were performed on a feed containing 10,150 ppm NaCl which flowed through a 2.26 cm I.D. by 61 cm long seamless cellulose acetate membrane similar to the one that we have used. Their membrane was wrapped in nylon parchment and then inserted into a solid metal support tube which contained several small perforations to permit product withdrawal (that is, the procedure of Loeb, 1966). The test section of Richardson et al. was preceded by a 30.4-cm long piece of 1.02-cm I.D. tube. Hence, an uncertain degree of hydrodynamic development was attained at the inlet.

Table 3 lists the additional operating parameters and fluid property data employed by Richardson et al. We note that, for lack of any other information, the membrane constants were assumed to be uniform throughout the test section's length. K_1 and K_3 were obtained by us using the procedures described earlier. Accordingly, we used the overall product rate and product composition data for the largest Reynolds number reported ($Re = 19{,}284$) for calibration purposes.

The theoretical model employed here for analyzing the laminar Re runs of the Philco-Ford group is similar to that used for estimating the tube length for the onset of combined free and forced convection. That is, from Equation (18) we calculated X_{tr} for the operating conditions under consideration so that the dimensional transition length x_{tr} could be determined for each inlet Reynolds number, that is, $x_{tr} = (X_{tr})\ (Re)\ (Sc)\ (d_H)$. For $x < x_{tr}$, the UWF Leveque (forced convection) Sherwood number expression was used to calculate local V_w and C_p, while for $x > x_{tr}$, we used a Siegwarth et al. type (combined free and forced convection) of Sherwood number relationship with $C_1 = 0.42$ [see Equation (15a)]. This choice of C_1 appeared to give the optimum predictions—it is not very much different from the values determined from our own experiments given by Equations (16) and (17). Additionally, in order to show the poorer agreement attainable by neglecting buoyancy effects, the forced convection model was applied to the entire test section length.

The local $|V_w|$ and C_p values were integrated numerically over the 61 cm test length and converted to the same units as given by Richardson et al. The reults are compared in Table 3 where it can be seen that there is significantly better agreement between experiment and our model (which includes buoyancy effects) than there is for a model based on forced convection alone. Perhaps even better agreement might have been obtained had there existed a fully developed laminar profile at the test section inlet. It is likely that some turbulence was present for the run at $Re = 2{,}143$ since this was near the transi-

tion Reynolds number and, as mentioned earlier, a sudden diameter expansion existed near the membrane's inlet. Consequently, one would expect that the observed product rate and composition values would be greater than predicted. Also, we note that the Sh expression used for the combined free and forced convection calculations was assumed to be independent of Re whereas our own experiments indicate a small decrease at Re around 540. Had we employed a smaller value of C_1, say $C_1 = 0.40$, for the theoretical predictions at $Re = 429$, this would have resulted in closer agreement with the data. Nevertheless, the results shown in Table 3 tend to support the findings of the present work.

The UC Davis group used a commercial membrane tubule (Calgon-Havens) of length 220 cm and inside diameter 1.27 cm for concentrating a sucrose feed. The tubule was preceded by a 1-m long pipe of 0.94-cm inside diameter (Monge et al., 1973). Operating pressure and feed composition were fixed at 500 lb./sq. in. gauge (3.45 MN/m^2) and 15 wt. % sucrose, respectively. This represents a situation where the feed's osmotic pressure is 40% of the applied pressure, that is, concentration polarization should have a marked influence on V_w. Isothermal test runs were performed at 25°, 35°, and 45°C for several feed rates and the total amount of water removed was measured and reported as a length-averaged permeation velocity. For all feed Re, the experimental values of V_w were significantly greater than predicted by forced convection models (by as much as 100% at $Re \lesssim 100$). Furthermore, except for say $Re \lesssim 100$, the experimental V_w was insensitive to feed Re. This behavior suggests that combined free and forced convection was the dominant mass transfer mechanism throughout most of the tube length.

We have used the calculation scheme described earlier to predict permeation rates for the conditions and membrane properties reported by the UC Davis group (Merson, 1973). We have only considered the data obtained at 25°C since this represents the largest feed Re range. Physical property data was obtained from Monge (1972). Since sucrose solutions have concentration-dependent properties (viscosity increases strongly while diffusivity decreases moderately as concentration increases), the question thus arises of how to account for variable ν and D. We have used, perhaps, the simplest means, that is, properties were based on C_o for $x < x_{tr}$ and on C_w for $x > x_{tr}$. Goldsmith (1971) reported good success with this assumption in correlating data on ultrafiltration of high molecular weight organic solutes.

In Table 4 we have listed the values of V_w obtained experimentally together with those predicted by a forced convection model applied over the entire membrane length and a combined free and forced convection model applied for $x > x_{tr}$. Note that a proportionality constant of $C_1 = 0.4$ was used to obtain the best fit. This value is approximately the same as found for the NaCl-H_2O system even though the Schmidt number for sucrose is approximately five times greater. The good agreement between our predictions and the data is readily apparent and adds further support to our findings. It should be realized, too, that the forced-convection only model, since it used ν_o and D_o, would have yielded even poorer agreement had concentration dependence been taken into account.

Table 4. Comparison of UC Davis Data (Merson, 1973) with Predictions of Forced Convection Models Which Neglect or Include Buoyancy Effects

Membrane properties: II $K_1 = 1.07 \times 10^{-6}$ cm/s · lb./sq.in.
III $K_1 = 1.12 \times 10^{-6}$ cm/s · lb./sq.in.
$K_3 \simeq 0$ assumed for both membranes
Sc = 2795 (based on feed properties at $T = 25$°C)
$\zeta = 0.41$ (Hodgman 1962)

Feed rate,* cm^3/min.	Reynolds number, Re	Permeation Velocity, cm/min. FC+ only	FC followed by CFFC++	Exp't.	x_{tr}, cm
290 (II)	369	3.86	6.56	6.41	10
385 (III)	490	4.20	6.71	6.7	14
425 (II)	541	4.27	6.59	6.50	14
540 (II)	687	4.53	6.44	6.69	18
620 (III)	789	4.76	6.76	6.9	20
910 (III)	1157	5.25	6.81	7.15	30
1305 (III)	1660	5.73	6.97	7.2	42

* Numeral in parentheses designates membrane code of Kennedy et al. (1973).
† FC = forced convection, that is, $Sh = 1.301\ (d_H \cdot Pe/x)^{1/3}$.
†† CFFC = combined free and forced convection, that is, $Sh = 0.40\ Ra_w^{1/4}$.

ACKNOWLEDGMENT

The authors are indebted to Prof. R. L. Merson of the University of California, Davis, for making available to us, prior to publication, the sucrose data. Helpful information relating to membrane handling techniques was supplied by Dr. John L. Richardson and Mr. Clarke H. Lewis of Philco-Ford Corporation, Newport Beach, Calif. This work was sponsored in part by NSF Grant K034380 and by the Office of Saline Water (U.S Department of the Interior).

NOTATION

C_1 = proportionality coefficient in Sherwood number correlation for combined free and forced convection
C = solute mass fraction
D = molecular diffusion coefficient, cm^2/s
d_H = hydraulic diameter, cm
Gr_D = Grashof number for mass transfer, $g\zeta d_H^3(C_w - C_o)/\nu^2$
g = gravitational acceleration, 980 cm/s^2
$gpdsf$ = gallons per day per square foot
j_s = diffusive flux of solute, g/(cm^2·s)
K_1 = membrane's pure water permeability constant, cm/(s·lb./sq.in.)
K_3 = membrane's solute permeability constant, cm/s
K_5 = osmotic pressure proportionality constant, psi/(solute mass fraction)
k = mass transfer coefficient in absence of transverse wall velocity, cm/s
k^* = mass transfer coefficient in presence of transverse wall velocity, cm/s
n_s = net solute flux at membrane surface, g/(cm^2·s)
ΔP = applied pressure drop across membrane, lb./sq. in. or MN/m^2
Pe = Peclet number, $Re \cdot Sc$
Pe_w = wall Peclet number, $-|V_w|d_H/D$
R = membrane's solute rejection parameter, $(1 - C_p/C_w)$
Ra = Rayleigh number, $Gr_D \cdot Sc$
Re = Reynolds number, $U_m d_H/\nu$
Sc = Schmidt number, ν/D
Sh = Sherwood number in absence of transverse wall velocity, kd_H/D
Sh^* = Sherwood number in presence of transverse wall velocity, $k^* d_H/D$

T = temperature, K
UWF = designates uniform wall flux boundary condition
U_m = average axial velocity, cm/s
V = local transverse component of velocity, cm/s
X_{tr} = dimensionless axial distance, $x_{tr}/(d_H \cdot Pe)$
x = axial distance, cm
x_{tr} = distance at which buoyancy effects become significant, cm
y = transverse distance from membrane surface, cm

Greek Letters

α = thermal diffusivity, cm^2/s
β = volumetric expansion coefficient due to temperature change, $\left| -\frac{1}{\rho}\frac{\partial \rho}{\partial T} \right|, K^{-1}$
ν = kinematic viscosity, cm^2/s
ρ = solution density, g/cm^3
θ_{AB} = correction factor for finite interfacial velocity, Sh'/Sh
ϕ_{AB} = rate factor, $V_w d_H/(D \cdot Sh)$
ζ = volumetric expansion coefficient due to concentration change, $\left| -\frac{1}{\rho}\frac{\partial \rho}{\partial C} \right|$
π = osmotic pressure (a function of solute concentration, C), lb./sq.in.
$\Delta\pi$ = difference in osmotic pressure across membrane, $\pi_w - \pi_p$, lb. sq. in.

Subscripts

b = bulk or cup-mixing value
o = condition at conduit inlet or beyond diffusion film thickness
p = condition in product (ambient pressure) stream
w = condition at membrane/solution interface or at conduit wall

LITERATURE CITED

Bergles, A. E., and R. R. Simonds, "Conbined Forced and Free Convection for Laminar Flow in Horizontal Tubes with Uniform Heat Flux," *Intern. J. Heat Mass Transfer*, **14**, 1989 (1971).

Bird, R. B., W. E. Stewart, and E. N. Lightfoot, "Transport Phenomena," Wiley, New York (1960).

Brian, P. L. T., "Mass Transport in Reverse Osmosis", in *Desalination by Reverse Osmosis*, U. Merten, (ed.), The M.I.T. Press, Cambridge, Mass. (1966).

Deissler, R. G., "Analysis of Turbulent Heat Transfer, Mass Transfer, and Friction in Smooth Tubes at High Prandtl and Schmidt Numbers," NACA Rept. 1210 (1955).

Derzansky, L. J., "A Theoretical Analysis of Turbulent Hyperfiltration (Reverse Osmosis) in Tubes with Particular Application to Water Desalination," M.S. thesis, Clarkson College of Technology, Potsdam, New York (1968).

———., "An Experimental Study of Reverse Osmosis in a Horizontal Tube: Combined Free and Forced Convection", Ph.D. thesis, Clarkson College of Technology, Potsdam, New York (1973).

Gill, W. N., and M. Scher, "A Modification of the Momentum Transport Hypothesis," *AIChE J.*, **7**, 61 (1961).

Gill, W. N., C. Tien, and D. W. Zeh, "Analysis of Continuous Reverse Osmosis Systems for Desalination," *Intern. J. Heat Mass Transfer*, **9**, 907 (1966a).

Gill, W. N., D. W. Zeh, and C. Tien, "Reverse Osmosis in Annuli," *AIChE J.*, **12**, 1141 (1966b).

Gill, W. N., L. J. Derzansky, and M. R. Doshi, "Convective Diffusion in Laminar and Turbulent Hyperfiltration (Reverse Osmosis) Systems," in *Surface and Colloid Science*, E. Matijevic, (ed.), Vol. 4, 261-360, Wiley-Interscience, New York (1971).

Grethlein, Hans E., "A Study on Reproducibility of Cellulose Acetate Membranes," *Desalination*, **12**, 45 (1973).

Goldsmith, Robert L., "Macromolecular Ultrafiltration with Microporous Membranes," *Ind. Eng. Chem. Fundamentals*, **10**, 113 (1971).

Hendricks, T. J., J. F. Macquin, and F. A. Williams, "Observations on Buoyant Convection in Reverse Osmosis," *ibid.*, **11**, 276 (1972).

Hodgman, C. D., (Ed.), *Handbook of Chemistry and Physics*, 44th Edit., Chemical Rubber, Cleveland, Ohio (1962).

Johnson, Jr., J. S., L. Dresner, and K. A. Kraus, "Hyperfiltration (Reverse Osmosis)," in "Principles of Desalination," K.S. Spiegler, (Ed.), Academic Press, Inc., New York (1966).

Kennedy, T. J., L. E. Monge, B. J. McCoy, and R. L. Merson, "Concentrating Liquid Foods by Reverse Osmosis: The Problems of Polarization and High Osmotic Pressure," *AIChE Symp. Ser. No. 132*, **69**, 81 (1973).

Kesting, R. E., "Synthetic Polymeric Membranes," McGraw-Hill, New York (1971).

Kimura, S., and S. Sourirajan, "Mass Transfer Coefficients for Use in Reverse Osmosis Process Design," *Ind. Eng. Chem. Process Design Develop.*, **7**, 539 (1968).

Knudsen, J. G., and D. L. Katz, *Fluid Dynamics and Heat Transfer*, McGraw-Hill, New York (1958).

Lacey, R. E., and S. Loeb, (Eds.), *Industrial Processing with Membrane*, Wiley, New York (1972).

Loeb, S., "A Composite Tubular Assembly for Reverse Osmosis Desalination," *Desalination*, **1**, 35 (1966).

Merson, R. L., private communication (June 6, 1973).

Merten, U., H. K. Lonsdale, and R. L. Riley, "Boundary-Layer Effects in Reverse Osmosis," *Ind. Eng. Chem. Fundamentals*, **3**, 210 (1964).

Merten, U., (Ed.), *Desalination by Reverse Osmosis*, The M.I.T. Press, Cambridge, Mass. (1966).

Mikesell, R. D., "The Effect of Heat Transfer on the Flow in a Horizontal Pipe," Ph.D. thesis, Univ. of Illinois, Urbana (1963).

Monge, Luis E., "Reverse Osmosis: Effect of Heating the Boundary Layer on the Permeation Rate," M.S. thesis, Univ. California, Davis (1972).

Monge, L. E., B. J. McCoy, and R. L. Merson, "Improved Reverse Osmosis Permeation by Heating," *J. Food Sci.*, **38**, 633 (1973).

Newell, P. H., and A. E. Bergles, "Analysis of Combined Free and Forced Convection for Fully Developed Laminar Flow in Horizontal Tubes," *J. Heat Transfer, Trans. ASME, Ser. C*, **92**, 83 (1970).

Ramanadhan, K., and W. N. Gill, "Combined Forced and Free Convective Diffusion in Vertical Semipermeable Parallel Plate Ducts," *AIChE J.*, **15**, 872 (1969).

Richardson, J. L., G. Segovia, W. Baerg, and M. Anderson, "Reverse Osmosis Tubular Module Optimization," Office of Saline Water, U.S. Dept. of the Interior, Res. Develop. Rept. No. 455 (1969).

Shannon, R. L., and C. A. Depew, "Combined Free and Forced Laminar Convection in a Horizontal Tube with Uniform Heat Flux," *J. Heat Transfer, Trans. ASME, Ser. C*, **90**, 353 (1968).

Shaw, R. A., R. DeLuca, and W. N. Gill, "Reverse Osmosis: Increased Productivity by Reduction of Concentration Polarization in Laminar Flow Reverse Osmosis Using Intermediate Non-Rejecting Membrane Sections," *Desalination*, **11**, 189 (1972).

Sherwood, T. K., P. L. T. Brian, and R. E. Fisher, "Desalination by Reverse Osmosis," *Ind. Eng. Chem. Fundamentals*, **6**, 2 (1967).

Siegwarth, D. P., R. D. Mikesell, T. C. Readal, and T. J. Hanratty, "Effect of Secondary Flow on the Temperature Field and Primary Flow in a Heated Horizontal Tube," *Intern. J. Heat Mass Transfer*, **12**, 1535 (1969).

Sourirajan, S., *Reverse Osmosis*, Academic Press, New York (1970).

Srinivasan, S., C. Tien, and W. N. Gill, "Simultaneous Development of Velocity and Concentration Profiles in Reverse Osmosis Systems," *Chem. Eng. Sci.*, **22**, 417 (1967).

Thomas, David G., "Estimation of Concentration Polarization for Ion-Exclusion Hyperfiltration Membranes with Turbulent Flow," *Ind. Eng. Chem. Fundamentals*, **11**, 302 (1972).

Manuscript received January 25, 1974; revision received March 22 and accepted April 6, 1974.